

Ionic Strength Effects in Polyelectrolyte Brushes: The Counterion Correction

R. Hariharan,^{†,‡} C. Biver,[§] and W. B. Russel^{*,†}

Department of Chemical Engineering, Princeton University, Princeton, New Jersey 08544, and Elf Atochem, 95 Rue Danton, BP 108, 92300 Levallois-Perret, France

Received December 15, 1997; Revised Manuscript Received June 19, 1998

ABSTRACT: We propose a means of accounting for the contribution of counterions to the ionic strength within a polyelectrolyte brush, which is then incorporated into models treating the effects of electrostatic interactions, chain stretching, and curvature on the layer thickness for chains attached to a spherical particle. Combining an electrostatic wormlike chain model originated by Odijk, Fixman, and co-workers with the blob model of Daoud and Cotton predicts without adjustable parameters the layer thickness for a wide range of ionic strengths and particle radii. A simplified scaling version that neglects stiffening due to electrostatic interactions greatly underestimates the layer thickness but captures the dependence on ionic strength reasonably.

1. Introduction

This paper follows up on the preceding experimental paper¹ and a brief earlier theoretical one² dealing with polyelectrolyte brushes. The former presents data for polyelectrolyte diblocks adsorbed from a selective solvent to demonstrate the effects of ionic strength and curvature and interprets the ionic strength dependence through a simplified blob model. The latter correlates the effect of curvature from micelles to flat surfaces by combining the Daoud–Cotton model with the electrostatic wormlike chain theory, originated by Odijk, Fixman, and co-workers^{3,4} to account for chain stiffening and excluded volume. The analysis of data^{1,5} for colloidal particles and micelles was restricted to relatively high added salt concentrations ($0.016 \text{ M} \leq C_a \leq 1 \text{ M}$) by our assumption that the ionic strength in the brush equals that in the bulk solution. When the added salt concentration is low, the counterions from the polymer backbone contribute significantly to the local ionic strength, as expected from Donnan equilibrium, for example. In this paper, we accomplish this correction in a mean field sense and incorporate the results into the simplified and detailed electrostatic blob models mentioned above to cover the full range of ionic strengths.

We begin by briefly summarizing the key steps and conclusions of the previous versions of the model (section 2) and then explain (section 3) the method for correcting the ionic strength within the brush for counterions. This is then incorporated into the blob models (section 4) to predict layer thicknesses of polyelectrolyte brushes composed of diblock copolymers on colloidal particles or in micelles. The predictions are tested for a wide range of curvatures (2.8–156 nm) and ionic strengths (7×10^{-6} to 1 M). Section 5 highlights the key findings.

2. A Brief Review

The Daoud–Cotton model⁶ envisions a sphere of radius R surrounded by p chains that form radial strings of volume-filling blobs. Each blob has a cross-sectional

area ξ^2 that increases with radial position r to remain equal to the area per chain $4\pi r^2/p$. The number of segments per blob N_ξ increases with the size according to the Flory relation $\xi = l_k N_\xi^{3/5} (v/l_k^3)^{1/5}$ with l_k the electrostatic Kuhn length and v the excluded volume. The layer thickness L is simply the distance required to accumulate N_k electrostatic segments per chain,

$$\left(\frac{L}{R} + 1\right)^{5/3} - 1 = \frac{kL_c(\sigma v)^{1/3}}{R(l_k)} \quad (1)$$

with $L_c = N_k l_k$ the contour length of the polymer chain, $\sigma = p/4\pi R^2$ the chain density, and $k = O(1)$ a constant. Our earlier papers show this to account reasonably well for curvature in polyelectrolyte brushes at high ionic strengths.^{1,2} In the following, we recap the assumptions invoked to estimate l_k and v .

The electrostatic wormlike chain theory, originally proposed for individual polyelectrolyte chains in solution,^{3,4} should be appropriate for local stiffening and excluded volume interactions inside a blob, provided the interactions remain pairwise. Strictly speaking this requires the electrostatic screening length to be shorter than the blob size, which is the correlation length normally associated with excluded volume interactions. The sizes of the blobs are bounded by those at the inner (ξ_i) and outer (ξ_o) edges of the layer, which are estimated by considering them to be at $r = R + \xi_i/2$ and $R + L - \xi_o/2$, respectively. Therefore, $4R/(\sqrt{p} - 2) \leq \xi \leq 4(R + L)/(\sqrt{p} + 2)$. Treating the Debye length κ^{-1} ($\approx 0.3 \text{ nm}/\sqrt{C_s}$) to be the electrostatic screening length constrains the ionic strength as $C_s > [5.8 \times 10^{-3} \text{ M} (\sqrt{p} - 2)^2/R^2]$ in water with R in nanometers.

As in neutral polymer solutions, the interactions experienced by a monomer on a polyelectrolyte chain have contributions from both adjacent and distant neighbors along the backbone. Steric hindrance and electrostatic repulsion among neighbors result in chain stiffening. The former depends primarily on the molecular architecture and determines the bare or intrinsic Kuhn length l , but the latter is a strong function of the ionic strength and can cause remarkable changes in chain stiffness. Distant portions of a chain interact via

* Author to whom all correspondences should be addressed.

[†] Current address: Polymer Materials Laboratory, General Electric CR&D, Schenectady, NY 12301.

[§] Elf Atochem.

electrostatic, van der Waals, and steric forces, which are normally lumped into the excluded volume or binary cluster integral v . To calculate these, we adopt the version of the electrostatic wormlike chain theory developed by Davis and Russel,⁸ which predicts the radius of gyration and second virial coefficients of dilute solutions of potassium poly(styrenesulfonate) in KCl quantitatively over a broad range of ionic strengths.

Depicting a section of the polyelectrolyte backbone as a charged torus and solving the nonlinear Poisson–Boltzmann equation yields the electrostatic free energy of bending. Balancing the sum of the electrostatic and steric hindrance energies against the kinetic energy kT determines the increased stiffness due to electrostatic interactions l_k/l as a function of the ionic strength and the distance l_c between charges along the backbone. The binary cluster integral (v/l_k^3) is calculated for a pair of cylinders of length l_k and radius a . The electrostatic contribution depends strongly on l_k and weakly on l_k/l_c and $a\kappa$.

In our previous paper, l_k and v were taken from Davis and Russel⁸ for poly(styrenesulfonate) at the ionic strengths of interest. The core radii for micelles are available from experimental measurements,^{1,5,7} while particle radii were reported from TEM. The theory was then tested for relatively high ionic strengths ($0.016 \text{ M} \leq C_a \leq 1 \text{ M}$) by plotting $[(L/R + 1)^{5/3} - 1]$ versus $[L_c(v\sigma/l_k)^{1/3}/R]$ and noting that all the data fall about the expected straight line.

In the full model the electrostatic Kuhn length and excluded volume are rather complex functions of ionic strength and charge density. Neglecting the effect of electrostatics on chain stiffness and approximating the excluded volume as that for hard rods of radius $1/\kappa$,

$$v \sim l_k^2 \kappa^{-1} \quad (2)$$

produces from eq 1 a simplified model with a dependence on the added electrolyte concentration for roughly planar layers, $L \sim C_s^{-1/6}$, that conforms reasonably well with data for particles of modest curvature. In the limit of zero radius, the model predicts $L \sim C_s^{-1/10}$, which comes close to the measured value for micelles.^{1,2}

3. Counterion Correction to the Ionic Strength in the Brush

A full field theory would predict self-consistently the positions of the segments and the electric fields, naturally accounting for the ion distributions relative to the bulk solution through the nonlinear Poisson–Boltzmann equation. The electrostatic wormlike chain theory, however, assumes the electrostatic interactions to be local and additive, breaking the coupling between the local ion concentrations and those in the bulk. Thus, the Debye length κ^{-1} , which affects both l_k and v , depends on the *local* ionic strength within a blob in the brush, which may differ from that in the bulk. The difference, in effect, derives from the counterions associated with the fixed charges on the polymer backbone. When the concentration of added salt is low, the counterions become significant.

We relate the concentrations of free ions n_i of charge ez_i in the brush to that in the bulk n_i^∞ using the Boltzmann distribution

$$n_i = n_i^\infty \exp\left(-\frac{ez_i\bar{\psi}}{kT}\right) \quad (3)$$

determined by $\bar{\psi}$ the mean electrostatic potential in the layer. For simplicity, we ignore the spatial variation in the charge density and electrostatic potential, and choose to work with the mean values within the layer. The brush is assumed to be electrically neutral, which implies that the positive charge in the backbone should equal the negative charge from the counterions:

$$\bar{\rho}_f = -\sum_i ez_i n_i \quad (4)$$

where

$$\bar{\rho}_f = \frac{1}{V} \int_V \rho_f dV = \frac{3eR^2\sigma L_c}{l_c[(R+L)^3 - R^3]} \quad (5)$$

is the volume-averaged fixed charge density. The neutrality should apply when the charges in the polyelectrolyte brush far exceed the surface charge and when the layer thickness considerably exceeds the Debye length. Equations 3 and 4 can now be solved to obtain the mean potential, which then determines the effective ionic strength in the brush.

For a symmetric electrolyte with $z_+ = -z_- = z$ and $n_+^\infty = n_-^\infty = n^\infty$, eq 4 reduces to

$$\bar{\rho}_f = en^\infty \left[\exp\left(\frac{ez\bar{\psi}}{kT}\right) - \exp\left(-\frac{ez\bar{\psi}}{kT}\right) \right] \quad (6)$$

which has the solution

$$\exp\left(-\frac{ez\bar{\psi}}{kT}\right) = \left[1 + \left(\frac{\bar{\rho}_f}{2en^\infty} \right)^2 \right]^{1/2} - \frac{\bar{\rho}_f}{2en^\infty} \quad (7)$$

The “effective” ionic strength in the brush is related to the number density of ions by

$$C_s = \frac{1}{2} \sum_i \frac{n_i z_i^2}{N_a} \quad (8)$$

which upon simplification via eqs 3 and 7 reduces to

$$C_s = \frac{n^\infty}{N_a} \left[1 + \left(\frac{\bar{\rho}_f}{2en^\infty} \right)^2 \right]^{1/2} = C_a \left[1 + \left(\frac{\bar{\rho}_f}{2ezN_a C_a} \right)^2 \right]^{1/2} \quad (9)$$

where C_a is the added salt concentration and C_s is the local ionic strength (both in molar units). The second term in brackets represents the contribution due to counterions. An alternate formulation would involve applying the Poisson–Boltzmann equation for a radially varying electrostatic potential and ionic strength. However, the spatially varying fixed charge density couples the effective Debye length and the electrostatic parameters v and l_k to the layer thickness in a complicated fashion and entails an iterative procedure. The overall solution derived above greatly simplifies the problem, without losing the essential features.

The full model now consists of eq 1, relating the layer thickness to the core radius, the density of chains, and the characteristics of the chains; eq 9 relating the Debye length to the density of fixed charges and the bulk electrolyte concentration; and the Davis and Russel

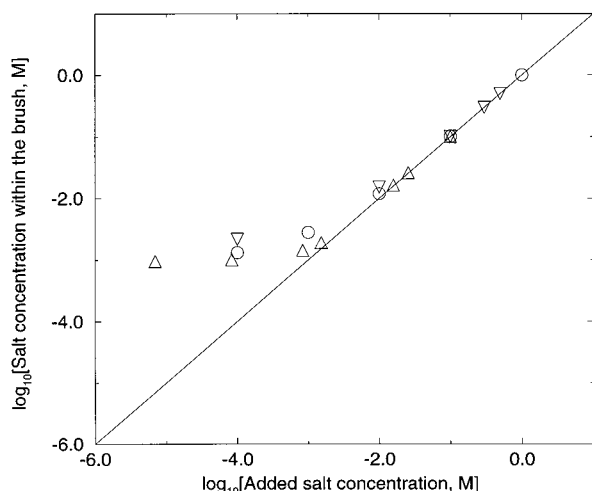


Figure 1. Relationship between salt concentration within the brush (C_s) and added salt concentration (C_a), as predicted from eq 9. The straight line corresponds to a neutral brush and the symbols to polystyrene particles coated by PtBS-NaPSS diblock copolymer chains (circle), MT3 micelles (triangle up) and MT2 micelles (triangle down).

model⁸ relating ν and l_k to the Debye length and the spacing l_c of charges along the backbone.

4. Results and Discussion

Coated colloidal particles and micelles examined earlier^{1,2} are analyzed over the full experimental range of ionic strength to test the ability of this more detailed treatment to predict the layer thickness. Alternatively, we can invert eq 1 to plot the apparent values of (ν/l_k) extracted from the measurements as a function of ionic strength. The previous papers^{1,2} contain more details on the experimental systems and calculations.

4.1. Counterion Correction. Examining the relationship between the concentration of salt within (C_s) and outside the polyelectrolyte brush (C_a), requires estimation of the effective number of fixed charges in the layer. For this, we apply the linear electrostatic theory for polyelectrolyte solutions,⁹ popularly called the “counterion condensation” theory, which predicts

$$\left(\frac{l_b}{l_{c,\text{eff}}}\right) = \begin{cases} l_b/l_c & l_b \leq l_c \\ 1 & l_b > l_c \end{cases} \quad (10)$$

Since the Bjerrum length l_b is defined as the distance at which the interaction energy of a pair of electrons equals kT , the result implies that counterions “condense” on the backbone whenever the energy of interaction of a pair of backbone charges exceeds kT . Upon condensation, the charges are no longer “effective”. For charges spaced out farther than l_b , no condensation occurs. The nonlinear theory⁶ predicts $(l_b/l_{c,\text{eff}})$, which differs from the linear result (eq 10) by $\pm 40\%$ at the ionic strengths and charge densities of interest. The fraction of sulphonated monomers is close to unity for all the polyelectrolyte brushes we examine, implying $l_c = 0.252$ nm. Since this value is much lower than the Bjerrum length (0.7 nm), we set $l_c = (l_{c,\text{eff}}) = l_b$.

Figure 1 shows the results of our calculations for the adsorbed diblocks and the MT2 and MT3 micelles based on the measured dimensions and the specified molecular masses, aggregation numbers or adsorbed amounts, and degrees of sulfonation. For high salt concentra-

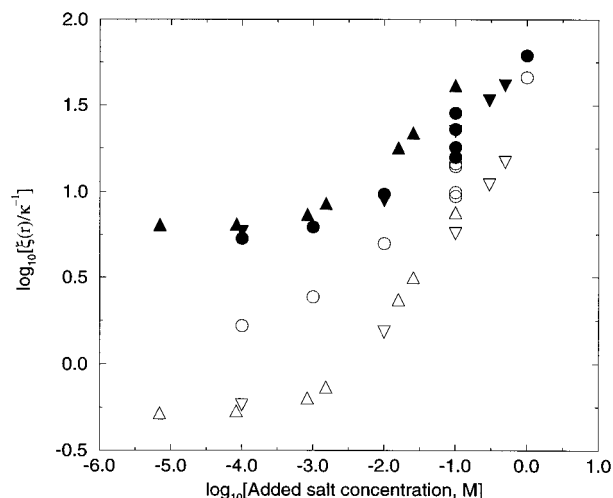


Figure 2. Comparison of blob size at core (unfilled symbols) and the outer edge (filled symbols) against the Debye length to check validity of model. The systems examined are: PtBS-NaPSS diblocks on polystyrene particles (circle) and in micelles of MT3 (triangle up) and MT2 (triangle down).

tions, the counterions are negligible, resulting in $C_s \approx C_a$. However, as the added salt concentration decreases, C_s departs significantly from C_a , approaching a limit as $C_a \rightarrow 0$ of

$$C_s = \frac{\bar{\rho}_f}{2ezN_a} \quad (11)$$

As the concentration of added salt varies from 7×10^{-6} to 1 M, we expect from eq 9 that the concentration inside the brush changes only from 10^{-3} to 1 M. No measurements exist for the ion concentrations in the brush, but accurate calculation of l_k and ν at low ionic strengths depends on these estimates. Therefore, our ability to predict the thickness of the polyelectrolyte brush layer thickness will serve as a test of the validity of eq 9.

This is an appropriate point to assess whether the blobs are large relative to the Debye length, which we stated at the outset as one criterion for the validity of this model. Figure 2 displays the range of $\xi\kappa$ as a function of added salt for each of the three systems. Note that the blobs for the chains adsorbed onto the polystyrene latices and the outermost blobs for the micelles always satisfy the assumption. The inner blobs for the micelles do so only at the higher ionic strengths, so the model may suffer for the micelles at 10^{-2} M or lower. Similar trends are also obtained when we compare the size of blobs to l_k ; their ratio varies from 3–30 at the outermost layer to 0.1–1.0 at the inner layer. Nonetheless, we feel comfortable with the model since the larger blobs comprise the bulk of the layer and thereby determine the layer thickness L .

4.2. Comparison with Experimental Data. The effect of the counterion correction on the predicted layer thickness is shown in Figures 3 and 4. Without the correction, i.e., when $C_s = C_a$, reasonable agreement with experiments is observed for the higher ionic strengths ($C_a \geq 1.6 \times 10^{-2}$ M) as reported previously and represented here by the unfilled symbols in Figure 3. In sharp contrast, the data for lower ionic strengths (filled symbols) lie well above the prediction represented by the straight line of slope unity through the origin. This is consistent with Figure 1, which demonstrated the counterion correction to be unimportant at ionic

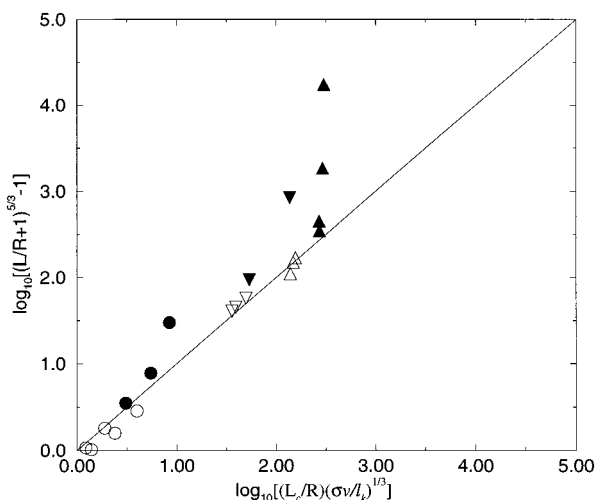


Figure 3. Comparison of the model with $C_s = C_a$ (solid line) with data from PtBS-NaPSS diblocks on polystyrene particles (circle) and in micelles of MT3 (triangle up) and MT2 (triangle down). The unfilled symbols refer to our previous study, which restricted attention to higher ionic strengths ($C_a \geq 1.6 \times 10^{-2}$) and the filled symbols to lower ionic strengths. Together, the data spans core radii from 2.8 to 155.5 nm, and ionic strengths from 7×10^{-6} to 1 M.

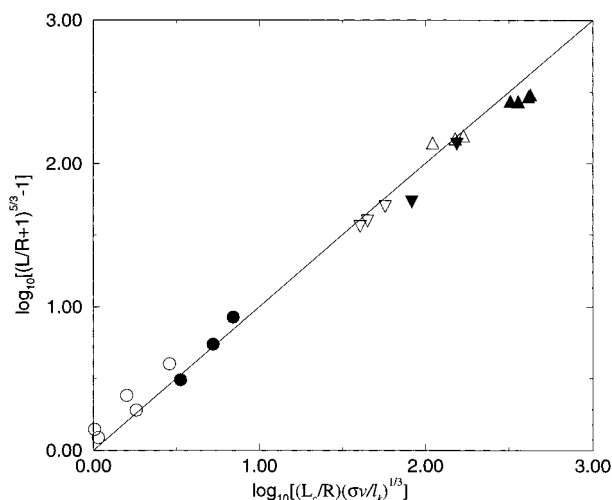


Figure 4. Comparison of the full model incorporating the correction for counterions (solid line) with the same experimental data.

strengths above 10^{-3} M but crucial for lower values. Not surprisingly, the largest departure (nearly 2 orders of magnitude) between theory and experiments is found for the MT3 micelles at the lowest ionic strength.

Employing the counterion correction (Figure 4) produces a dramatic improvement in the agreement between theory and experiments at low ionic strengths. The form of the plot belies the broad range of the data, which covers $0.7 < L/R < 29$ and $\Delta L/L = 1.7\text{--}4.2$. While approximate, the theory is entirely predictive, with all the parameters needed by the model known from independent measurements for each experimental system.

4.3. Predictions of the Excluded Volume. The treatment of the data in Figure 4 displays the combined effects of excluded volume, chain stiffness, and curvature on the layer thickness. To decouple the curvature effect, based on the Daoud–Cotton idea of radially swelling blobs, from estimates of v and l_k through the electrostatic wormlike chain model, eq 1

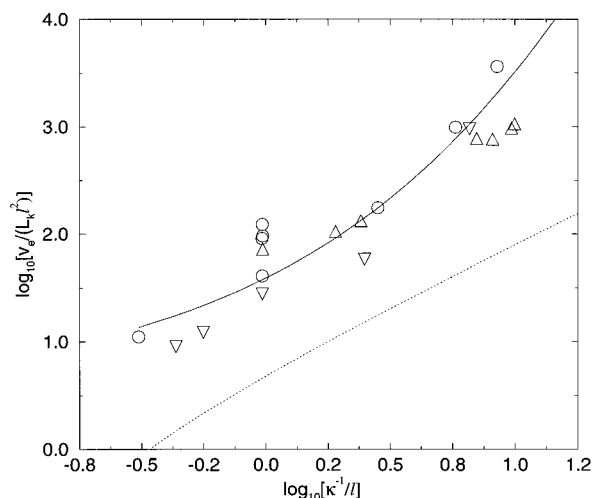


Figure 5. Comparison of the value of $v/(l_k l^2)$ extracted from the same data as in the previous figures with predictions from the simplified model (dotted line) and the full electrostatic wormlike chain theory (solid line).

can be rewritten as

$$\left(\frac{v}{l_k l^2}\right)^{1/3} = \frac{R}{L_c(l^2 o)^{1/3}} \left[\left(\frac{L}{R} + 1\right)^{5/3} - 1 \right] \quad (12)$$

This separates the measured quantities on the right-hand side from those predicted with electrostatic wormlike chain theory on the left. Thus, values of layer thickness, core radius, aggregation number and contour length serve to estimate an “experimental” value of $v/(l_k l^2)$ to be compared against the predictions.

For the full theory, we employ the v and l_k from Davis and Russel,⁸ while the simplified version sets $l = l_k$ and neglects the van der Waals attraction such that

$$\frac{v}{l_k l^2} = 2 \frac{R(w)}{l_k} \quad (13)$$

with $R(w)$ from Skolnick and Fixman¹⁰ and

$$w = \frac{2\pi}{l_b \kappa (a\kappa)^2} \left(\frac{l_b}{l_c}\right)_{\text{eff}}^2 \left[\frac{\exp(-a\kappa)}{K_1(a\kappa)} \right]^2 \quad (14)$$

from Davis and Russel.⁸ Here K_1 is the modified Bessel function and $[l_b/l_c]_{\text{eff}}$ is the effective charge density after correcting for nonlinearities in the Poisson–Boltzmann equation. $R(w)$ is a relatively weak function but does vary significantly over the range of interest. Both models require the ionic strength within the brush as corrected for counterions (eq 9).

Figure 5 compares the data against the predictions of the full and simplified models as a function of $1/\kappa l$ with ionic strength decreasing from left to right. The Daoud–Cotton treatment collapses data from all systems to the same order of magnitude for a given ionic strength. The prediction from the simplified model is almost a straight line, despite the complex dependence of $R(w)$ on ionic strength. This justifies our assuming $R(w)$ to be independent of ionic strength previously.¹ Though the trend is reasonable, this simplified approximation greatly underpredicts the experimental values for $v/(l_k l^2)$. Thus incorporation of eq 2 into the Daoud–Cotton model should err quantitatively on the layer thickness but describe changes with salt concen-

tration appropriately, consistent with our earlier result¹ for extreme values of the core radii.

The full model predicts the qualitative trend and the values of $v/(l_k \ell^2)$ as a function of salt concentration within the scatter of the data. Thus the combination of the electrostatic wormlike chain theory, with accurate accounting for electrostatic nonlinearities and the presence of counterions, with the Daoud–Cotton blob model should serve as an excellent tool for estimating the layer thickness of polyelectrolyte brushes as a function of ionic strength, adsorbed amount, and core radius. The accuracy, however, comes at the expense of somewhat complex models for l_k and v . In sharp contrast, the simplified model makes gross assumptions in ignoring chain stiffening and the dependence of excluded volume on charge density but succeeds in predicting qualitatively the dependence on salt concentration.

5. Conclusions

The detailed electrostatic blob model presented here incorporates a mean-field correction for counterions, a geometrical treatment of curvature, and interactions between neighboring and distant segments along the backbone through an electrostatic Kuhn length and excluded volume, respectively. With independently measured values of all the relevant parameters the theory predicts the layer thickness over a broad range of ionic strengths and radii of curvature within the scatter in the measurements for poly(styrenesulfonate)/

poly(*tert*-butylstyrene) diblocks on polystyrene latices and in micelles. A simplified version that neglects chain stiffening and adopts a constant prefactor in the excluded volume greatly underestimates layer thickness and v/l_k but captures qualitatively the dependence on ionic strength.

Acknowledgment. The authors would like to thank Patrick Guenoun, Guy Chauveteau, and Matthew Tirrell for many insightful discussions. Elf Aquitaine, Elf Atochem, and the National Science Foundation through NSF/CTS-9107025 and the MRSEC/DMR-9400362 are gratefully acknowledged for their financial support.

References and Notes

- (1) Hariharan, R.; Biver, C.; Mays, J.; Russel, W. B. *Macromolecules* **1998**, *31*, 7506.
- (2) Biver, C.; Hariharan, R.; Mays, J.; Russel, W. B. *Macromolecules* **1997**, *30*, 1787.
- (3) Odijk, T.; Houwaart, A. C. *J. Polym. Sci., Polym. Phys.* **1978**, *16*, 627.
- (4) Fixman, M.; Skolnick, J. *Macromolecules* **1978**, *11*, 863.
- (5) Guenoun, P.; Davis, H. T.; Tirrell, M.; Mays, J. W. *Macromolecules* **1996**, *29*, 3965.
- (6) Daoud, M.; Cotton, J. P. *J. de Phys. (Paris)* **1982**, *43*, 531.
- (7) Hariharan, R. Ph.D. dissertation, Princeton University, 1996.
- (8) Davis, R. M.; Russel, W. B. *J. Polym. Sci., Polym. Phys. Ed.* **1986**, *24*, 511.
- (9) Manning, G. S. *J. Chem. Phys.* **1969**, *51*, 924.
- (10) Skolnick, J.; Fixman, M. *Macromolecules* **1977**, *10*, 944.

MA9718199